ChemComm

Accepted Manuscript

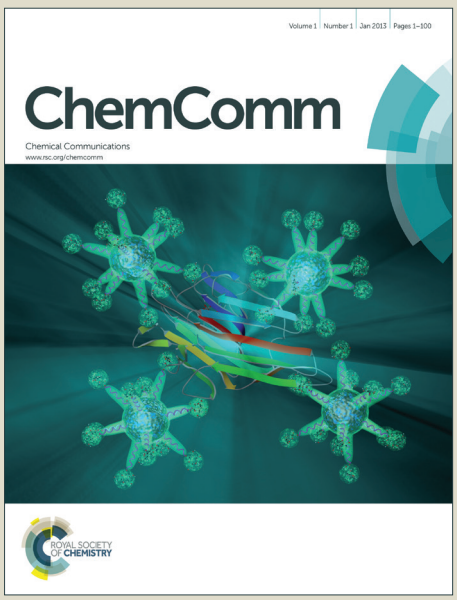

ROYAL SOCIETY OF CHEMISTRY

www.rsc.org/chemcomm

Journal Name

COMMUNICATION

Insight into the molecular dynamics of guest cation confined in deformable azido coordination frameworks†

Received 00th January 20xx,
Accepted 00th January 20xx

DOI: 10.1039/x0xx00000x

www.rsc.org/

Zi-Yi Du,*[a,b] Yu-Zhi Sun,[a] Shao-Li Chen,[b] Bo Huang,[b] Yu-Jun Su,[b] Ting-Ting Xu,[a] Wei-Xiong Zhang,*[b] and Xiao-Ming Chen[b]

The molecular dynamics of encapsulated cation within perovskite-like coordination polymers $[(CH_3)_3NH][M(N_3)_3]$ (M = Mn, Cd) are investigated, which are well controlled by the confined space of a deformable azido framework. The Mn-based compound provides a rare example that features unvaried/varied rotational energy barrier during its two different structural phase transitions.

Molecule-based inclusion compounds containing rotatable or motionable guest component, as an interesting host–guest model, have attracted considerable attention in the field of modern optoelectronic materials, owing to their sensitive and controllable responses to external stimuli, such as thermal, pressure, light, or electricity.[1-9] As one type of coordination-based inclusion compounds, the coordination polymers (CPs) with perovskite structure are quite unique and have promising application as new dielectric and ferroelectric materials.[7,10-20] These perovskite-like CPs, with inclusion of rotatable or motionable guest cations into the well-matched cage-like host frameworks (For exemplified structural diagram, see Scheme 1), are apt to undergo displacive-type or order–disorder-type phase transitions upon thermal stimulus. It has been found that their related physical properties primarily depend on the molecular dynamics of the guest cations. Therefore, understanding the motion modes or the rotational rate of the guest cations is critical for the practical application of such perovskite-like CPs. However, investigations on the guest dynamics within these CPs remain very scarce.[13,14,17]

Recently, we have studied a perovskite-like CP encapsulating polar dimethylammonium cation, namely $[(CH_3)_2NH_2][Cd(N_3)_3]$ (**1**).[21] It was revealed that the molecular dynamics of the $[(CH_3)_2NH_2]^+$ cation can be well controlled by the variable confined space of the host framework, and the varied motion modes of the $[(CH_3)_2NH_2]^+$ cation accompanying with a synergistic deformation of the $[Cd(N_3)_3]^-$ framework lead to a structural phase transition at around 174 K. Up to now, although some perovskite-like azido CPs had been reported by us[21-22] and others[23-24], the detailed guest dynamics among them were scarcely investigated. It was thus of interest for us to explore the guest molecular dynamics of other two related perovskite-like azido CPs, with the polar dimethylammonium guest being replaced by a larger and heavier trimethylammonium cation, namely $[(CH_3)_3NH][Mn(N_3)_3]$ (**2**) and $[(CH_3)_3NH][Cd(N_3)_3]$ (**3**). Our current studies show that **2** is a rarely observed example that features unvaried/varied rotational energy barrier during its two different structural phase transitions, and the comparison of the guest molecular dynamics within these perovskite-like azido CPs provides valuable informations for modulating the guest molecular dynamics in the confined space.

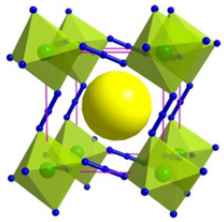

Scheme 1 Deformable cage unit enclosed by eight octahedrally coordinated metal ions and twelve end-to-end bridging azido ligands, which encapsulate a guest cation.

Compound **2** was prepared according to a reported procedure,[24] and it can undergo two reversible structural phase transitions above room temperature. Upon heating, the space group of its three phases changes from $P2_1/c$ (**2α**), to $C2/c$ (**2β**), and then to R-3m (**2γ**), with the phase transition temperatures (T_C) being *ca.* 332 and 360 K, respectively. Although the crystal structures of **2** and the related phase transitions have been briefly described by Wang and coworkers,[24] here, for a deep discussion of the guest molecular dynamics, we supplemented some characterizations for **2** and

[a] College of Chemistry and Chemical Engineering, Gannan Normal University, Ganzhou 341000, China. E-mail: ziyidu@gmail.com
[b] MOE Key Laboratory of Bioinorganic and Synthetic Chemistry, School of Chemistry and Chemical Engineering, Sun Yat-Sen University, Guangzhou 510275, China. E-mail: zhangwx6@mail.sysu.edu.cn

† Electronic Supplementary Information (ESI) available: Experimental details, characterizations for **2** and **3**, and crystal structure analysis for **2**. CCDC 1054930 and 1054931. For ESI and crystallographic data in CIF or other electronic format, see DOI: 10.1039/x0xx00000x

performed a more detailed analysis on its phase transitions and crystal structures (see ESI,† Section II).

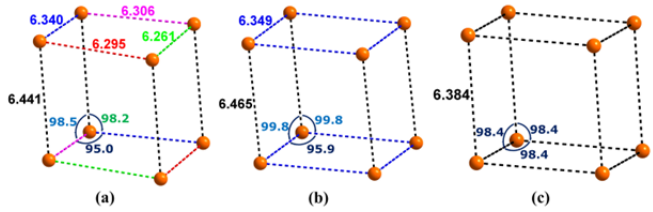

Fig. 1 The Mn···Mn distances (Å) and Mn···Mn···Mn angles (°) within a $[Mn(N_3)_3]^-$ cage unit of **2α** at 298 K (a), **2β** at 350 K (b), and **2γ** at 360 K (c). The geometries are drawn based on the supplementary crystallographic data of reference 24.

It is noted that the monoclinic unit-cell parameters vary very slightly from **2α** to **2β** phase [*a*, *b*, *c* (Å), *β* (°): "8.464(6), 9.324(5), 12.882(7), 105.466(14) at 298 K" versus "8.502(16), 9.431(17), 12.93(2), 104.77(2) at 350 K"], whereas the lattice type changes from a primitive to a *C*-centered Bravais lattice.[24] The small difference between the two phases is consistent with the small thermal anomaly detected by the DSC measurement. For such phase transition, the total symmetric elements of the crystallographic point group remain unchanged (ESI,† Fig. S2), *i.e.* 4 (E, C_2, i, σ_h). However, the asymmetric unit changes from [$0 \le x \le 1$; $0 \le y \le 1/4$; $0 \le z \le 1$] to [$0 \le x \le 1/2$; $0 \le y \le 1/2$; $0 \le z \le 1/2$]. As for the transition from **2β** to **2γ**, the total symmetric elements of the crystallographic point group increase from 4 (E, C_2, i, σ_h) to 12 (E, $2C_3$, $3C_2$, i, $2S_6$, $3\sigma_v$). Thus, this transition should be ferroelastic with an *Aizu* notion of $\bar{3}m$F2/*m*,[25] and the number of equivalent unique ferroelastic directions is 3. In short, the former phase transition is characterized by a change of the lattice type but without the alteration of its crystal system, whereas the latter is a ferroelastic one characterized by a change of the crystal system. As indicated by the varied Mn···Mn distances and especially the Mn···Mn···Mn angles (Fig. 1), the deformation of the $[Mn(N_3)_3]^-$ framework in the latter transition is more remarkable than that in the former one. In addition, the Mn···Mn edges tend to be identical as the phase transition occurs, *i.e.*, the numbers of different $d_{Mn\cdots Mn}$ within a cage unit reduce from 5 (**2α**) to 2 (**2β**), and to 1 (**2γ**).

The driving force for phase transition **2α→2β** is mainly thought to be the disorder of the $[(CH_3)_3NH]^+$ guest. For an order–disorder transition, from the Boltzmann equation, $\Delta S = R\ln(N)$, where R is the gas constant and N represents the ratio of the numbers of respective geometrically distinguishable orientations in both phases. According to the single-crystal X-ray diffraction studies on the ordered and two-fold disordered $[(CH_3)_3NH]^+$ cation before and after the phase transition, the theoretical value of N should be 2 and thus the expected ΔS should be 5.8 $J\cdot K^{-1}\cdot mol^{-1}$. However, the ΔS value (1.5 $J\cdot K^{-1}\cdot mol^{-1}$) estimated from the C_P measurement (Fig. S4) is about one quarter of the expected value. This result shows that much residual entropy is left over, implying a significant relaxor character for this phase transition.[26] On the other hand, the driving force for **2β→2γ** can mainly be ascribed to the deformation of the $[Mn(N_3)_3]^-$ framework and the synchronous change in the rotation modes of the $[(CH_3)_3NH]^+$ guest. For this phase transition, the evaluated ΔS (3.4 $J\cdot K^{-1}\cdot mol^{-1}$, see ESI,† Fig. S4) is about 59% of the excepted value for the disordered $[(CH_3)_3NH]^+$ cations (two-fold → four-fold disorder), showing that some residual entropy is still left over at this stage.

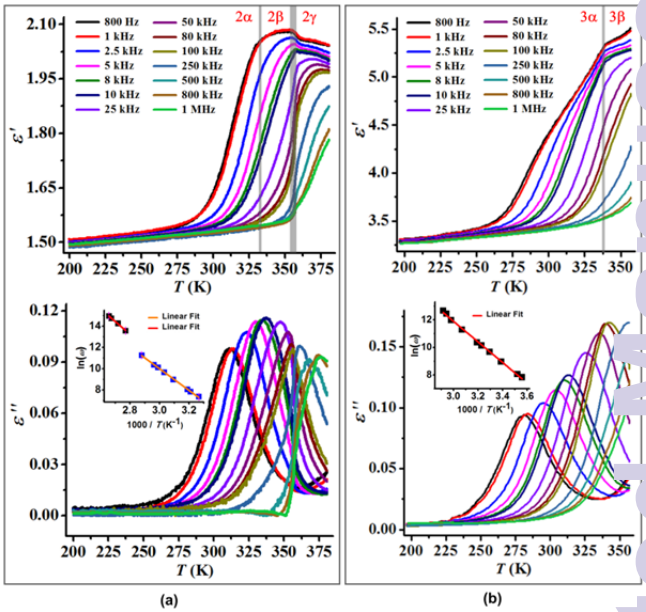

Fig. 2 Temperature-dependent ε' and ε'' at various ac frequencies for powder-pressed pellet samples of **2** (a) and **3** (b). The inset plots are shown in Arrhenius representation providing the linear fitting of ln(ω) versus $1/T_{peak}$.

Since the guest $[(CH_3)_3NH]^+$ cation is bestowed on a specific dipole moment, the change in the dynamical state of such cation should be reflected in the dielectric property of **2**. The above-discussed dynamical rotation of the guest cation and the relaxor character of such phase transition were unambiguously disclosed by the variable-temperature dielectric spectroscopy. As shown in Fig. 2a, the temperature-dependent complex dielectric permittivity ($\varepsilon = \varepsilon' - i\varepsilon''$) was measured at a broad band ranging from 800 Hz to 1 MHz and could be roughly divided into two regions: **2α**+**2β** and **2γ** (labeled as ***A***, ***B*** region, respectively), between which the value of ε' under all measured frequencies shows an obvious mutation at the T_C of **2β↔2γ**.

At region ***A***, ε' increased steadily from *ca.* 275 K to 356 K under all measured frequencies, *e.g.*, ε' at 100 kHz increased from 1.52 at 275 K to 1.85 at 356 K. Moreover, both the ε' and ε'' show notably frequency dependence, suggesting the dynamical feature of a polar rotator in **1**.[27-30] The peak maxima of ε'' were found at the rising temperatures (T_{peak}) from 305.2 to 347.4 K for the increasing f "0.5 → 25 kHz". Based on the Debye-type relaxation process, ε'' is strongly dependent on the temperature (T) and the angular frequency (ω) of the test field: $\varepsilon''(T) = \omega\tau(T)/[1 + \omega^2\tau(T)^2]$, where $\tau(T)$ is a temperature-dependent relaxation time obeying Arrhenius law: $1/\tau = \omega_0 \exp[-E_a/(k_B T)]$ (E_a is an activation energy, ω_0 is a pre-exponential factor, and k_B is the Boltzmann constant). The ε'' value reaches a maximum when $\omega\tau(T) = 1$. Thus, the test frequency can be used to estimate the rotational rate ($1/\tau$) at

T_{peak}, and then, an ω_0 value of 4.20 × 10^{17} s^{-1} and an E_a of 20.1 kcal·mol^{-1} (0.87 eV) were obtained from the plot of $1/T_{peak}$ versus ln(ω) (Fig. 2a, inset). It is worthy of note that the rotational energy barrier hardly varied after the phase transition of **2α→2β**, which may be mainly ascribed to the hardly distorted confined space constructed by the host framework during **2α→2β**. As a result, the observed variable-temperature dielectric constant ε' of **2** does not show a distinguishable inflection point at the T_C of **2α→2β**. Such phenomenon can also be explained by the significant residual entropy below T_C, as discussed above.

At region ***B***, the values of ε' below 100 kHz decreased slightly upon heating whereas those above 250 kHz showed an opposite shifting trend and increased steadily upon heating, strongly implying that dielectric relaxation still occurs at this region. Based on the frequency dependence of the ε'' value, in which T_{peak} for region ***B*** were found at 361.1, 367.8, 374.2 and 376.4 K for f = 250, 500, 800 and 1000 kHz, respectively, ω_0 and E_a values were estimated as 2.53 × 10^{20} s^{-1} and 23.9 kcal·mol^{-1} (1.04 eV), respectively (Fig. 2a, inset). The ω_0 value at region ***B*** is about three orders of magnitude of that at region ***A***, whereas the E_a value is slightly increased, implying that the guest molecular dynamics change slightly after the ferroelastic phase transition.

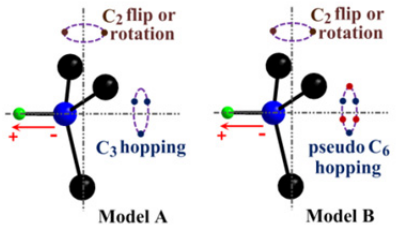

Fig. 3 Proposed rotation models for the triimethyl ammonium cation in **2β** (model A) and **2γ** phase (model B), respectively.

According to the recent studies on the molecular dynamics of the $[(CH_3)_2NH_2]^+$ cation in two types of confined space constructed by the perovskite-like $[KCo(CN)_6]^{2-}$ or $[Cd(N_3)_3]^-$ framework,[14,21] we proposed the possible rotation models for the $[(CH_3)_3NH]^+$ cation at **2β** and **2γ** phases (Fig. 3). In model A, a 120° flip about the electric dipole C_3 axis does not change the orientation of the dipole moment and should be thus dielectrically inactive. Whereas the rotation around the axis perpendicular to the dipole C_2 axis of the cation changes the orientation of dipole moment and is thus dielectrically active. For model B, the 120° flip about the electric dipole C_3 axis turns to a 60° one, while the rotation around the axis perpendicular to the dipole C_2 axis still exists. Notably, the dielectrically-active molecular dynamics of $[(CH_3)_3NH]^+$ cations are well confined by the deformable anionic $[Mn(N_3)_3]^-$ framework *via* supramolecular interactions (*e.g.*, ionic interaction and hydrogen bonds) in **2β** and **2γ** phases, leading to the remarkable dielectric relaxation behavior in a broad frequency region.

In order to get a deeper understanding on the encapsulated guest molecular dynamics discussed above, we synthesized a new perovskite-like azido CP, *i.e.*, **3**, which is cadmium analogue of **2** (For experimental details and Caution statement, see the ESI†). The TGA analysis shows that it starts decomposing at 98 °C under a nitrogen atmosphere (ESI,† Fig. S5), and a modulated differential scanning calorimeter (MDSC) measurement indicates that it undergoes a reversible second-order phase transition at T_C of 336 K (see ESI,† Section III and Fig. S6), which is slightly higher than that (332 K) of **2**. Structural analysis reveals that **3** is isomorphic to **2** in both **α** and **β** phases (ESI,† Table S1), except that **2β** can further transform to a $R\bar{3}m$ phase at a higher temperature. The ΔS value (1.7 J·K^{-1}·mol^{-1}) of **3α→3β** estimated from the C_P measurement is roughly the same as that of **2** (ESI,† Fig. S7). It is believed that if **3** decomposes at a higher temperature, then a second similar phase transition may be expected.

The variable-temperature dielectric spectroscopy was also measured for **3** to detect its guest molecular dynamics. As shown in Fig. 2b, both of the [ε' − T] and [ε'' − T] curves show similar variations to those in "**2α+2β**". An analogous relaxation process can also be uncovered by the frequency dependence of ε'', in which the peak maxima were found at the T_{peak} ranging from 281.0 to 342.8 K for f "0.8 → 100 kHz". Thus an ω_0 value of 7.89 × 10^{14} s^{-1} and an E_a of 14.8 kcal·mol^{-1} (0.64 eV) can be evaluated (Fig. 2b, inset). The E_a remains unvaried during **3α→3β**, which is similar to that during **2α→2β**. However, the E_a value here is about three-fourths in comparison with that of **2**, indicating that the interaction between the $[(CH_3)_3NH]^+$ guest and the cage-like anionic framework is somewhat weaker in **3**.

Considering that **3** features a similar $[Cd(N_3)_3]^-$ host framework to **1** and has a same $[(CH_3)_3NH]^+$ guest component as **2**, the comparisons among them are very meaningful:

(i) All three compounds exhibit dielectric relaxation, owing to the dielectrically active rotation of the encapsulated polar guest cations within them. When the E_a value is somewhat high (*e.g.* 14.8 kcal·mol^{-1} (0.64 eV) for the $[(CH_3)_3NH]^+$ cation in **3**), an orientationally ordered (frozen) state of the guest cation can be achieved as the temperature decreases to a certain extent. However, if the E_a value is low enough, *e.g.* 2.00/8.64 kcal·mol^{-1} (0.09/0.38 eV) for the $[(CH_3)_2NH_2]^+$ cation in **2** before/after the structural phase transition, a "rotating or hopping" (melt-like) state of the guest cation can still exist even at a very low temperature. The larger E_a value of **3** can be mainly ascribed to the heavier weight and larger size of the guest $[(CH_3)_3NH]^+$ cation. For **2**, owing to a slightly smaller size of the cage unit whithin it (Fig. 1 and Fig. S8), the E_a value in **2** is somewhat larger than that in **3**, which means that the $[(CH_3)_3NH]^+$ cation in **2** rotates less easily than that in **3**. As a result, the dielectric response (ε') of **2** is smaller than that of **3**.

(ii) From the thermodynamic point of view, the phase transition types of **2α↔2β** (or **3α↔3β**) and **2β↔2γ** are second-order and first-order, respectively, which mean that the inherent phase transition mechanism of them differs essentially. In the former transition, the host framework distorted very slighlty, so the phase transition is mainly caused by the rotation of the guest cation, which has a hardly varied E_a value after the phase transition, and thus the observed variable-temperature dielectric constant ε' of **2** and **3** does not

show a distinguishable inflection point during **2α↔2β** and **3α↔3β**. On the other hand, the phase transition of **2β↔2γ** can be ascribed to the combined effect of a rotatable $[(CH_3)_3NH]^+$ guest and a deformable $[Mn(N_3)_3]^-$ framework, which leads to a change of the rotational energy barrier after the phase transition, and thus the observed temperature-dependent ε' manifests an obvious mutation at the T_C of **2β↔2γ**. For **1**, a notable deformation of the $[Cd(N_3)_3]^-$ framework cause a remarkable change of the rotational energy barrier during the phase transition, and thus leads to a rare sharp decrease of ε' from low-T to high-T phase.[21]

In summary, the molecular dynamics of encapsulated $[(CH_3)_3NH]^+$ cation were studied for perovskite-like CPs, *i.e.*, **2** and **3**. Compared with the $[(CH_3)_2NH_2]^+$ cation confined in the $[Cd(N_3)_3]^-$ framework of **1**, the $[(CH_3)_3NH]^+$ cation confined in the $[Mn(N_3)_3]^-/[Cd(N_3)_3]^-$ framework of **2**/**3** has a much higher rotational energy barrier (14.8 kcal·mol^{-1} (0.64 eV) for **3α** and **3β**, 20.1 kcal·mol^{-1} (0.87 eV) for **2α** and **2β**, and 23.9 kcal·mol^{-1} (1.04 eV) for **2γ**, respectively), which are well controlled by the variable confined space of a deformable host framework. Considering that the E_a value plays a crucial role for dielectric response, further research works will be devoted to modulating the E_a within new host-guest systems, for the exploitation of controllable and switchable dielectric materials.

Acknowledgements

This work was supported by the NSFC (21290173, 91422302 and 21301198), the 973 Project (2014CB845602), and NSF of Guangdong (S2012030006240). Z.-Y. D. is thankful to the NSFC (21361002), and NSF of Jiangxi (20151BAB203003).

Notes and references

‡ It is noted that the synthesis, crystal structure, phase transition and especially the magnetic bistability of **2** have been reported by Wang and coworkers previously.[24]

1 A. Müller, H. Reuter and S. Dillinger, *Angew. Chem. Int. Ed.*, 1995, **34**, 2328.
2 *Host–Guest Systems Based on Nanoporous Crystals*, (Eds: F. Laeri, F. Schüth, U. Simon and M. Wark), Wiley-VCH, Weinheim, 2003.
3 E. R. Kay, D. A. Leigh and F. Zerbetto, *Angew. Chem. Int. Ed.*, 2007, **46**, 72.
4 H. Jin, Y. Zheng, Y. Liu, H. Cheng, Y. Zhou and D. Yan, *Angew. Chem. Int. Ed.*, 2011, **50**, 10352.
5 X. Yan, F. Wang, B. Zheng and F. Huang, *Chem. Soc. Rev.*, 2012, **41**, 6042.
6 (a) F. Huang and L. Isaacs, Acc. Chem. Res., 2014, **47**, 1923; (b) J. Hu and S. Liu, *Acc. Chem. Res.*, 2014, **47**, 2084.
7 W. Zhang, Y. Cai, R.-G. Xiong, H. Yoshikawa and K. Awaga, *Angew. Chem. Int. Ed.*, 2010, **49**, 6608.
8 (a) Y. Zhang, H.-Y. Ye, D.-W. Fu and R.-G. Xiong, *Angew. Chem. Int. Ed.*, 2014, **53**, 2114; (b) H.-Y. Ye, S.-H. Li, Y. Zhang, L. Zhou, F. Deng and R.-G. Xiong, *J. Am. Chem. Soc.*, 2014, **136**, 10033.
9 (a) B. Qin, Z. Zhao, R. Song, S. Shanbhag and Z. Tang, *Angew. Chem. Int. Ed.*, 2008, **47**, 9875; (b) H. Tang, J. Wang, H. Yin, H. Zhao, D. Wang and Z. Tang, *Adv. Mater.*, 2015, **27**, 1117.
10 (a) Z. Wang, B. Zhang, T. Otsuka, K. Inoue, H. Kobayashi and M. Kurmoo, *Dalton Trans.*, 2004, 2209; (b) B. Zhou, Y. Imai, A. Kobayashi, Z.-M. Wang and H. Kobayashi, *Angew. Chem. Int. Ed.*, 2011, **50**, 11441.
11 P. Jain, N. S. Dalal, B. H. Toby, H. W. Kroto and A. K. Cheetham, *J. Am. Chem. Soc.*, 2008, **130**, 10450.
12 W. Li, A. Thirumurugan, P. T. Barton, Z. Lin, S. Henke, H. H.-L. Yeung, M. T. Wharmby, E. G. Bithell, C. J. Howard and A. K. Cheetham, *J. Am. Chem. Soc.*, 2014, **136**, 7801.
13 (a) D.-W. Fu, W. Zhang, H.-L. Cai, Y. Zhang, R.-G. Xiong, S. D. Huang and T. Nakamura, *Angew. Chem. Int. Ed.*, 2011, **50**, 11947; (b) X. Zhang, X.-D. Shao, S.-C. Li, Y. Cai, Y.-F. Yao, R.-G. Xiong, and W. Zhang, *Chem. Commun.*, 2015, **51**, 4568.
14 W. Zhang, H.-Y. Ye, R. Graf, H. W. Spiess, Y.-F. Yao, R.-Q. Zhu, and R.-G. Xiong, *J. Am. Chem. Soc.*, 2013, **135**, 5230.
15 Y. Takahashi, R. Obara, Z.-Z. Lin, Y. Takahashi, T. Naito, T. Inabe, S. Ishibashi and K. Terakura, *Dalton Trans.*, 2011, **40**, 5563.
16 T. Asaji, Y. Ito, J. Seliger, V. Žagar, A. Gradišek and T. Apih, *Phys. Chem. A*, 2012, **116**, 12422.
17 (a) M. Mączka, A. Pietraszko, B. Macalik and K. Hermanowicz, *Inorg. Chem.*, 2014, **53**, 787; (b) M. Mączka, A. Ciupa, A. Gągor, A. Sieradzki, A. Pikul, B. Macalik, and M. Drozd, *Inorg. Chem.*, 2014, **53**, 5260; (c) M. Mączka, A. Pietraszko, B. Macalik and A. Sieradzki, J. Trzmiel and A. Pikul, *Dalton Trans.*, 2014, **43**, 17075; (d) M. Mączka, B. Bondzior, P. Dereń, A. Sieradzki, J. Trzmiel, A. Pietraszko and J. Hanuza *Dalton Trans.*, 2015, **44**, 6871.
18 A. Kojima, K. Teshima, Y. Shirai and T. Miyasaka, *J. Am. Chem. Soc.*, 2009, **131**, 6050.
19 S. Kazim, M. K. Nazeeruddin, M. K. Nazeeruddin, M. Grätzel and S. Ahmad, *Angew. Chem. Int. Ed.*, 2014, **53**, 2812.
20 (a) H.-Y. Ye, Y. Zhang, D.-W. Fu and R.-G. Xiong, *Angew. Chem. Int. Ed.*, 2014, **53**, 11242; (b) L.-H. Kong, D.-W. Fu, Q. Ye, H.-Y. Ye, Y. Zhang and R.-G. Xiong, *Chin. Chem. Lett.*, 2014, **25**, 84[illegible]
21 Z.-Y. Du, T.-T. Xu, B. Huang, Y.-J. Su, W. Xue, C.-T. He, W.-X. Zhang and X.-M. Chen, *Angew. Chem. Int. Ed.*, 2015, **54**, 914[illegible]
22 (a) D Z.-Y. Du, Y.-P. Zhao, W.-X. Zhang, H.-L. Zhou, C.-T. He, W. Xue, B.-Y. Wang and X.-M. Chen, *Chem. Commun.*, 2014, **50**, 1989; (b) Z.-Y. Du, Y.-P. Zhao, C.-T. He, B.-Y. Wang, W. Xue, H.-L. Zhou, J. Bai, B. Huang, W.-X. Zhang and X.-M. Chen, *Cryst. Growth Des.*, 2014, **14**, 3903.
23 (a) F. A. Mautner, H. Krischner and C. Kratky, Monatsh. Chem., 1988, **119**, 1245; (b) F. A. Mautner, R. Cortes, L. Lezama and T. Rojo, *Angew. Chem. Int. Ed.*, 1996, **35**, 78[illegible] (c) S. Hanna, F. A. Mautner, B. Koppelhuber-Bitschnau and M. A. M. Abu-Youssef, *Mater. Sci. Forum*, 2000, **321-324**, 1098.
24 X.-H. Zhao, X.-C. Huang, S.-L. Zhang, D. Shao, H.-Y. Wei and X.-Y. Wang, *J. Am. Chem. Soc.*, 2013, **135**, 16006.
25 K. Aizu, *J. Phys. Soc. Jpn.*, 1969, **27**, 387.
26 (a) R. Samantaray, R. J. Clark, E. S. Choi, H. Zhou and N. S. Dalal, *J. Am. Chem. Soc.*, 2011, **133**, 3792; (b) R. Samantaray, R. J. Clark, E. S. Choi and N. S. Dalal, *J. Am. Chem. Soc.*, 2012, **134**, 15953.
27 *Broadband Dielectric Spectroscopy*, (Eds. F. Kremer and A. Schön-hals), Springer, Berlin, Germany, 2002.
28 S. Devautour-Vinot, G. Maurin, C. Serre, P. Horcajada, D. Paula da Cunha, V. Guillerm, E. de Souza Costa, F. Taulelle and C. Martineau, *Chem. Mater.*, 2012, **24**, 2168.
29 Q.-C. Zhang, F.-T. Wu, H.-M. Hao, H. Xu, H.-X. Zhao, L.-S. Long, R.-B. Huang and L.-S. Zheng, *Angew. Chem. Int. Ed.*, 2013, **52**, 12602.
30 P. Sippel, D. Denysenko, A. Loidl, P. Lunkenheimer, G. Sastre and D. Volkmer, *Adv. Funct. Mater.*, 2014, **24**, 3885.

Graphical Abstract

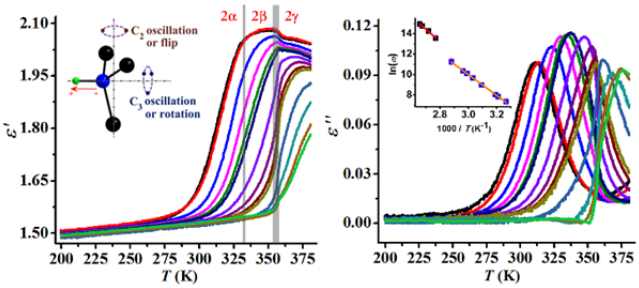

The guest molecular dynamics confined in deformable azido coordination frameworks are revealed, one of which features unvaried/varied E_a during its two structural phase transitions.